Detection and Quantification of the Evolution Dynamics of Apoptosis Using the PET Voltage Sensor ^{18}F-Fluorobenzyl Triphenyl Phosphonium

Igal Madar[1], Yi Huang[2], Hayden Ravert[1], Susan L. Dalrymple[2], Nancy E. Davidson[2], John T. Isaacs[2], Robert F. Dannals[1], and J. James Frost[1]

[1]Division of Nuclear Medicine, Russell H. Morgan Department of Radiology, Johns Hopkins Medical Institutions, Baltimore, Maryland; and [2]Sidney Kimmel Comprehensive Cancer Center, Johns Hopkins Medical Institutions, Baltimore, Maryland

Apoptosis is a key mechanism in numerous pathologies. However, there are no effective noninvasive means available for an early detection and quantitative assessment of evolution dynamics of the apoptotic process. Here, we have characterized the ability of the novel PET voltage sensor ^{18}F-fluorobenzyl triphenyl phosphonium (^{18}F-FBnTP) to quantify the time-dependent apoptotic action of the taxanes paclitaxel and docetaxel in vitro and in vivo. **Methods:** The duration-dependent treatment effect of paclitaxel on ^{18}F-FBnTP uptake was assayed in human MDA-MB-231 breast carcinoma cells. The expression of the proapoptotic Bax and antiapoptotic Bcl-2 mitochondrial proteins, release of the apoptogen cytochrome c, and activation of executioner caspase-3 were determined by Western blotting. The fraction of viable cells was determined using 3-(4,5-dimethylthiazol-2-yl)-2,5-diphenyltetrazolium bromide. The effect of docetaxel on ^{18}F-FBnTP and ^{18}F-FDG uptake in orthotopic prostate tumors in mice was compared. **Results:** ^{18}F-FBnTP cellular uptake in viable cells declined linearly with the increasing duration of paclitaxel treatment, from 3 to 24 h, and plateaued at 48 h. The extent of decrease of ^{18}F-FBnTP correlated strongly with the Bax-to-Bcl-2 ratio (R^2 = 0.83) and release of cytochrome c (R^2 = 0.92), but preceded in time the caspase-3 cleavage. The P-glycoprotein blocker verapamil did not interfere with ^{18}F-FBnTP cellular uptake. ^{18}F-FBnTP prostate tumor contrast was greater than ^{18}F-FDG prostate tumor contrast. Docetaxel caused a marked decrease (52.4%) of ^{18}F-FBnTP tumor uptake, within 48 h, whereas ^{18}F-FDG was much less affected (12%). **Conclusion:** The voltage sensor ^{18}F-FBnTP is a viable means for quantification of paclitaxel pharmacodynamics. ^{18}F-FBnTP permits the detection of paclitaxel apoptotic action in vivo earlier than does ^{18}F-FDG. ^{18}F-FBnTP may afford a novel approach for early detection and quantitative assessment of the cumulative-effect kinetics of proapoptotic drugs and conditions using PET.

Key Words: molecular biology; molecular imaging; PET; ^{18}F-fluorobenzyl triphenyl phosphonium; apoptosis; breast carcinoma cell line; taxanes

J Nucl Med 2009; 50:774–780
DOI: 10.2967/jnumed.108.061283

Received Dec. 23, 2008; revision accepted Jan. 22, 2009.
For correspondence or reprints contact: Igal Madar, Johns Hopkins Medical Institutions, 601 N. Caroline St., Baltimore, MD 21287.
E-mail: imadar@jhmi.edu

Apoptosis, the most common form of programmed cell death, is a universal phenomenon involved in the developmental stage and the etiology and pathology of many medical disorders, including HIV, diabetes, cancer, cardiovascular and degenerative diseases, organ failure, and normal aging (*1,2*). Apoptotic cell death is a key mechanism of action of several first-line anticancer drugs, including taxanes (*3–5*). The noninvasive assessment of apoptosis using a targeted imaging biomarker has been a long-standing goal.

The apoptotic signaling cascade offers several potential targets for noninvasive imaging using radionuclide molecular probes, including the elevated expression of proapoptotic Bcl-2 proteins, release of cytochrome c, and cleavage of caspases such as caspase-3. To date, the only imaging agent under clinical investigation is annexin V, which targets the externalization of membranous phosphatidyl serine (PS) (*6,7*). Annexin V may provide valuable information on whether a condition or agent (reperfusion, anticancer drug) triggers apoptotic signaling, but it suffers from inherent and important drawbacks. Because of the transient nature of PS exposure, annexin V may report the extent of apoptosis at the time of the measurement that might be preferred but not the cumulative-effect kinetics of the proapoptotic condition over time. Furthermore, PS externalization occurs over a limited time window, which may vary widely among individuals and treatment protocols (*8*). A molecular imaging probe capable of detecting apoptosis, which is not limited to a certain time window, might allow the monitoring of the kinetics of the apoptotic process in target tissue. This monitoring would permit better diagnosis of disease development and assessment of efficacy and pharmacodynamics of therapeutic drugs.

An alternative approach for the noninvasive detection of apoptotic cell death, which may address annexin V limitations, is the targeting of the collapse of mitochondrial

membrane potential ($\Delta\Psi_m$), a hallmark of the initiating phase of apoptosis (*9,10*). Mitochondria mediate the intrinsic pathway of apoptosis in many cell types by integrating and executing a wide spectrum of proapoptotic conditions and agents, such as oxidative stress and anticancer drugs (*2,5,9*). The release of apoptogens (e.g., cytochrome c and apoptosis-inducing factor) from the mitochondrial matrix to the cytosol is associated with permeabilization of the outer membrane and consequent collapse of $\Delta\Psi_m$ (*10,11*). Unlike the transient nature of PS exposure, $\Delta\Psi_m$ loss in target cells or tissue is an ongoing process. Hence, monitoring $\Delta\Psi_m$ could offer an effective strategy for quantification of the progressive impact and kinetics of proapoptotic factors.

In the present study, we characterized the efficacy of ^{18}F-fluorobenzyl triphenyl phosphonium (^{18}F-FBnTP), a novel $\Delta\Psi_m$-targeting PET compound (*12*) developed in our laboratory (*13*), to detect and quantify the dynamics of apoptosis induced by varying durations of exposure of human MDA-MB-231 breast carcinoma cells to the proapoptotic agent paclitaxel. ^{18}F-FBnTP cell-bound activity was correlated with critical checkpoints of apoptosis, including the expression of pro- and antiapoptotic proteins, release of the apoptogenic factor cytochrome c, and downstream activation of executioner caspase-3. In vivo, the effect of docetaxel on ^{18}F-FBnTP was studied in orthotopic prostate tumors and compared with ^{18}F-FDG.

MATERIALS AND METHODS

Materials and Solutions

^{18}F-FBnTP (specific radioactivity, 40.7–266.4 GBq/μmol [1,100–7,200 Ci/mmol]) was prepared as described previously (*13*). The standard loading solution for transport studies was Dulbecco's modified essential medium (DMEM) containing 5 mM *N*-(2-hydroxyethyl)piperazine-*N*′-(2-ethanesulfonic acid) (HEPES) and 1% fetal bovine serum (v/v), pH 7.4. Paclitaxel and docetaxel were a gift from Bristol-Myers/Squibb and Rhone Poulenc/Rorer, respectively. For all experiments, a concentrated paclitaxel solution (10 mM in dimethyl sulfoxide [DMSO], stored at 4°) was diluted in medium to the desired concentration. In each experiment, control cells were exposed to a DMSO concentration equivalent to the highest DMSO concentration present in the paclitaxel-treated cells. Verapamil was purchased from Sigma. The human breast carcinoma MDA-MB-231 and prostate LAPC4 cell lines were purchased from the American Type Culture Collection.

Paclitaxel Treatment and Transport Assays

One million cells were seeded into each 10-mm petri dish (Falcon) in 10 mL of DMEM supplemented with 5% fetal bovine serum, 2 mM glutamine, and 100 units of penicillin and streptomycin per milliliter. Cells were incubated at 37°C in a 5% CO_2 atmosphere. Paclitaxel (50 nM) was subsequently added, and cells were incubated for different times (3, 6, 24, and 48 h). For transport studies with ^{18}F-FBnTP, MDA-MB-231 cells were harvested by trypsinization, washed 3 times with cold phosphate-buffered saline (PBS), and counted in a Coulter counter. Cells were resuspended in loading buffer and transferred to Eppendorf microfuge tubes (10^6/mL). Microfuge tubes were placed in a 37°C water bath for 60 min before use.

Uptake assays were initiated by adding ^{18}F-FBnTP (0.5–5 nM) to the incubation buffer. Previous studies demonstrated a stable intracellular-to-extracellular uptake ratio in the range of incubation concentrations of 0.5–20 nM ^{18}F-FBnTP (*12*). The uptake was terminated by centrifugation (800 revolutions per minute, 5 min). Aliquots (100 μL) of the supernatant were then obtained, and the remaining solution was aspirated. Microfuge tubes were placed on dry ice, and their tips were cut off just above the pellet. The radioactivity of the pellet and supernatant was assayed together with a standard solution (1:1,000) in a γ-counter. Nonspecific binding was also assayed by counting radioactivity in empty microfuge tubes with the tips removed; radioactivity was always less than 2% of the total radioactivity. Radiotracer uptake per 10^6 cells was expressed as the accumulation ratio (%) calculated by dividing the radioactivity in the pellet by the total radioactivity (supernatant plus pellet).

The effect of the calcium blocker verapamil was examined by incubation of MDA-MB-231 cells (1×10^6 cell/mL) with the agent (3 μM) 60 min before the addition of 3–5 nM ^{18}F-FBnTP. Uptake assays were performed 60 min thereafter. Cell-bound activity was calculated as described above.

Paclitaxel Treatment and Western Blotting

MDA-MB-231 cells treated with 50 nM paclitaxel for 3, 6, 24, and 48 h were harvested by trypsinization and washed twice with PBS. Cellular protein was isolated using the protein-extraction buffer containing 150 mM sodium chloride, 10 mM Tris (pH 7.2), 5 mM ethylenediaminetetraacetic acid, 0.1% Triton X-100 (Dow), 5% glycerol, and 2% sodium dodecylsulfonate. Protein concentrations were determined using the Micro Protein Assay Kit (Pierce). Equal amounts of proteins (50 μg/lane) were fractionated using 12% sodium dodecylsulfonate–polyacrylamide gel electrophoresis (SDS-PAGE) and transferred to polyvinylidene difluoride membranes. The membranes were incubated with primary antibodies against Bcl-2, Bax, caspase-3, and cytochrome c (1:2,000; Santa Cruz Biotechnology). After being washed with PBS, the membranes were incubated with peroxidase-conjugated goat antimouse or antirabbit secondary antibody (1:3,000; DAKO Corp.), followed by enhanced chemiluminescence staining using the enhanced chemiluminescence system (Amersham Biosciences).

Detection of Cytochrome C Release

Cells treated with different concentrations of paclitaxel for the desired exposure time were harvested by trypsinization, washed with PBS, and subsequently incubated in 100 μL of permeabilization buffer (210 mM D-mannitol, 70 mM sucrose, 10 mM HEPES, 5 mM succinate, 0.2 mM ethylene glycol tetraacetic acid, and 100 μg of digitonin per milliliter [pH 7.2]) for 5 min. After centrifugation for 10 min at 14,000*g*, the supernatant with protein content was saved and protein concentrations were determined using the Micro Protein Assay Kit. Equal amounts of protein were fractionated using 12% SDS-PAGE and analyzed by Western blotting as described above.

3-(4,5-Dimethylthiazol-2-yl)-2,5-Diphenyltetrazolium Bromide (MTT) Survival Assays

MDA-MB-231 cells (5,000 per well) were plated in 96-well dishes and treated with the various concentrations of paclitaxel for different lengths of time. At the end of each time, 200 μL of

an MTT solution (1 mg/mL) (Sigma Chemical Co.), diluted in serum-free culture medium, were added to each well. The plates were incubated at 37°C in a 5% CO_2 atmosphere for 4 h, allowing viable cells to reduce the yellow tetrazolium salt into dark blue formazan crystals. At the end of the 4-h incubation, the MTT solution was removed and 200 μL of 1:1 (v/v) solution of DMSO-ethanol were added to each well to dissolve the formazan crystals. The absorbance in individual wells was determined at 540 nm.

Effect of Docetaxel on ^{18}F-FBnTP and ^{18}F-FDG Tumor Uptake in Mice

Prostate carcinoma cells (LAPC4; 10^7 in 0.1 mL of medium) were injected directly into the prostate of anesthetized nude mice ($n = 12$). Palpable tumors appeared within 2–3 wk. At 4 wk after inoculation, when the tumor reached 5–7 mm, docetaxel was administered via the tail vein (12.5 mg/kg) in 6 tumor-bearing mice. The remaining 6 untreated mice served as the control. ^{18}F-FBnTP and ^{18}F-FDG uptake assays were performed 48 h after treatment. Mice were fasted overnight before the uptake assays. ^{18}F-FBnTP and ^{18}F-FDG (925 kBq/0.2 mL [25 μCi/0.2 mL] saline) were administered intravenously, each to tumor-bearing mice with ($n = 3$) and without ($n = 3$) docetaxel treatment. At 60 min after administration, prostrate tumor and adjacent nontumor prostate tissue were excised together with selected organs and weighed; tissue radioactivity along with standards (1:100) was counted in a γ-counter.

Statistics

Data are expressed as mean ± SD of 2–3 independent studies. All of the experiments were plated in triplicate, and the results of the assays are presented as mean ± SD. The statistical difference between groups was analyzed using a 2-tailed t test and a P value of less than 0.05.

RESULTS

Time-Dependent Effect of Paclitaxel on ^{18}F-FBnTP Cellular Uptake

Cells were treated with 50 nM paclitaxel for 3, 6, 24, and 48 h. The exposure of cells to paclitaxel resulted in a decrease of ^{18}F-FBnTP cellular uptake. A significant decrease of ^{18}F-FBnTP uptake was detected as early as 6 h after the start of treatment (20% ± 6.8, $P < 0.05$), which intensified after 24 and 48 h of treatment (50% and 73%, respectively), compared with the control. The time-dependent decline in ^{18}F-FBnTP uptake strongly correlated with the duration of paclitaxel treatment ($R^2 = 0.97$) (Fig. 1).

To exclude the effect of paclitaxel-induced cell death, ^{18}F-FBnTP cell-bound activity was normalized to the fraction of viable cells as measured by MTT staining. Normalization to viable cells revealed biphasic kinetics of the time-dependent paclitaxel effect on ^{18}F-FBnTP cellular uptake. An intense decline of ^{18}F-FBnTP uptake was measured during the first 24 h, which slowed at 48 h of paclitaxel treatment (Fig. 1). Three hours of exposure to 50 nM paclitaxel resulted in a slight (10%) but insignificant ($P > 0.09$) decrease of ^{18}F-FBnTP cellular uptake.

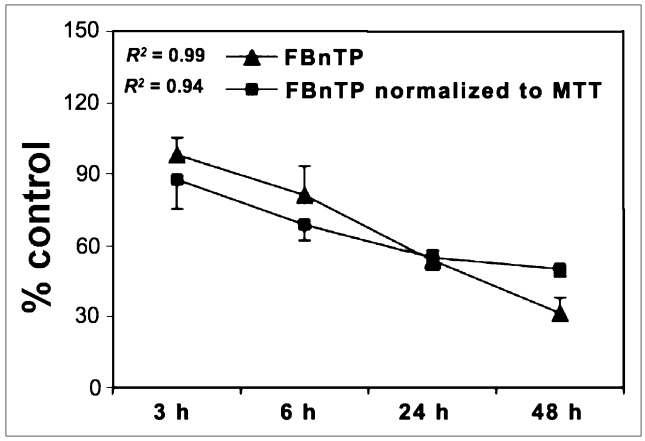

FIGURE 1. Effect of exposure to 50 nM paclitaxel on ^{18}F-BnTP uptake in MDA-MB-231 cells. ^{18}F-FBnTP cellular uptake decreases linearly with increasing duration of paclitaxel treatment. Correction to fraction of viable cells (MTT) shows that decrease of ^{18}F-FBnTP uptake plateaus at 48 h.

Correlation of ^{18}F-FBnTP Cellular Uptake with Markers of Apoptosis

The expression of the proapoptotic protein Bax, as assessed by Western blotting (Fig. 2A), increased with increasing duration of paclitaxel treatment (Fig. 2B). In contrast, the expression of the antiapoptotic protein Bcl-2 (Fig. 2A) slightly decreased with increasing treatment duration (Fig. 2B). ^{18}F-FBnTP cellular uptake decreased in proportion to the increase of the proapoptotic Bax expression (Fig. 2B). A strong linear correlation ($R^2 = 0.83$) was found between the percentage decrease of ^{18}F-FBnTP cell-bound activity and the ratio of Bax to Bcl-2 (Fig. 2C).

Treatment with paclitaxel resulted in an increase of release of cytochrome c to the cytosol (Fig. 3A). A significant increase of 21% ± 7.4% for paclitaxel-treated cells, compared with nontreated controls, was detected as early as 6 h after the start of paclitaxel treatment, which coincided in time with the earliest significant decrease of ^{18}F-FBnTP uptake. A strong direct time-dependent correlation ($R^2 = 0.92$) was found between the release of cytochrome c and the extent of decrease of ^{18}F-FBnTP cellular uptake (Fig. 3B).

Activation of caspase-3 significantly lagged behind the alteration in radiotracer uptake. Cleavage of caspase-3, as a percentage of control, remained stable until 24 h of treatment with paclitaxel (Fig. 4A). A significant increase of 25% ± 8.5% of caspase-3 cleavage was detected after 48 h of treatment, which paralleled a 52% ± 6.3% decrease of ^{18}F-FBnTP cellular uptake (Fig. 4B).

Effect of Verapamil

Possible interaction with the efflux protein P-glycoprotein (Pgp), which may contribute to the observed change in ^{18}F-FBnTP cellular uptake, was examined in the presence of the

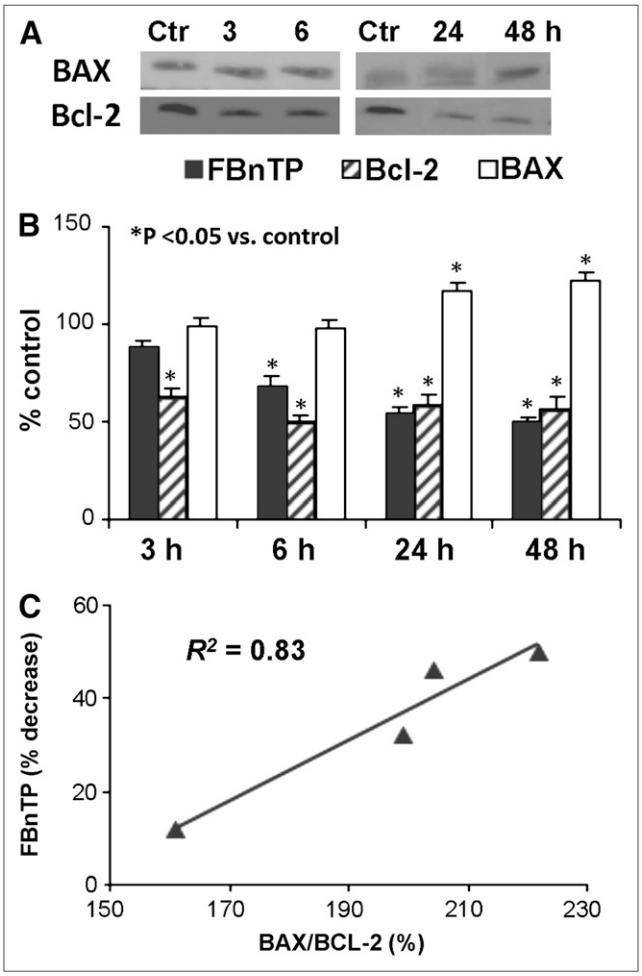

FIGURE 2. (A) Correlation of ^{18}F-FBnTP cellular uptake with expression of Bcl2 and Bax mitochondrial proteins. (B) Paclitaxel-induced time-dependent increase in Bax and decrease in Bcl2 expressions. (C) Percentage of decrease of ^{18}F-FBnTP cellular uptake strongly correlated with Bax-to-Bcl-2 ratio. Ctr = nontreated cells.

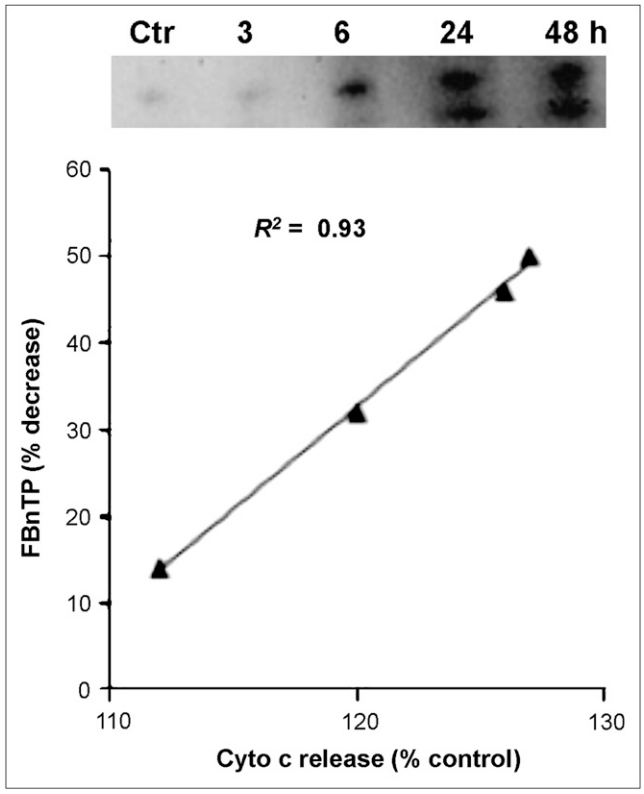

FIGURE 3. Correlation of ^{18}F-FBnTP cellular uptake and release of cytochrome c. (A) Paclitaxel treatment results in time-dependent increase of cytochrome c release to cytosol. (B) Percentage decrease of ^{18}F-FBnTP cellular uptake demonstrates strong linear correlation with cytochrome c release. Ctr = nontreated cells.

blocker verapamil. Cells treated for 24 and 48 h with paclitaxel were incubated with verapamil for 60 min before ^{18}F-FBnTP was added to the loading buffer. Verapamil, compared with the control, did not induce any significant effect on ^{18}F-FBnTP in either time group (Fig. 5).

Docetaxel Effect on ^{18}F-FBnTP and ^{18}F-FDG in Orthotopic Prostate Tumor

In nontreated mice, ^{18}F-FBnTP uptake (percentage injected dose per gram) in the prostate tumor was greater than ^{18}F-FDG uptake (mean ± SD, 1.84 ± 0.65 vs. 1.31 ± 0.14, respectively), but this difference was not statistically significant (P = 0.08) (Fig. 6A). However, ^{18}F-FBnTP uptake in the nonmalignant prostate parenchyma (0.62 ± 0.21) was significantly (P < 0.02) lower than that of ^{18}F-FDG (1.18 ± 0.78). Consequently, the tumor-to-prostate uptake ratio was significantly greater for ^{18}F-FBnTP than for ^{18}F-FDG (3.0 ± 0.46 vs. 1.63 ± 1.24, P = 0.009) (Fig. 6C).

Treatment with docetaxel for 48 h resulted in a decreased tumor uptake for ^{18}F-FBnTP (0.9 ± 0.31) and ^{18}F-FDG (1.15 ± 0.54) (Fig. 6B). The decrease of tumor uptake in docetaxel-treated mice, compared with prostate uptake in nontreated mice, was significantly stronger for ^{18}F-FBnTP (52.6%) than for ^{18}F-FDG (12.8%). This discrepancy between ^{18}F-FBnTP and ^{18}F-FDG decrease of uptake was maintained when tumor uptake was normalized to normal prostate tissue, which was collected from the same animal (55.4% vs. 15.3%) (Fig. 6C).

DISCUSSION

^{18}F-FBnTP is an accurate biomarker of cellular apoptosis in the breast cancer model. This finding is supported by the linear relationship between ^{18}F-FBnTP accumulation in viable cells and paclitaxel treatment duration. The tight linear correlation with critical checkpoints of apoptosis, including Bcl-2 protein expression and cytochrome c release, clearly indicates that the decline in ^{18}F-FBnTP cellular uptake is due to paclitaxel-induced apoptosis. These data support the concept of ^{18}F-FBnTP cell-bound activity as an effective correlate of the cumulative apoptotic action of paclitaxel. The in vitro findings are supported by

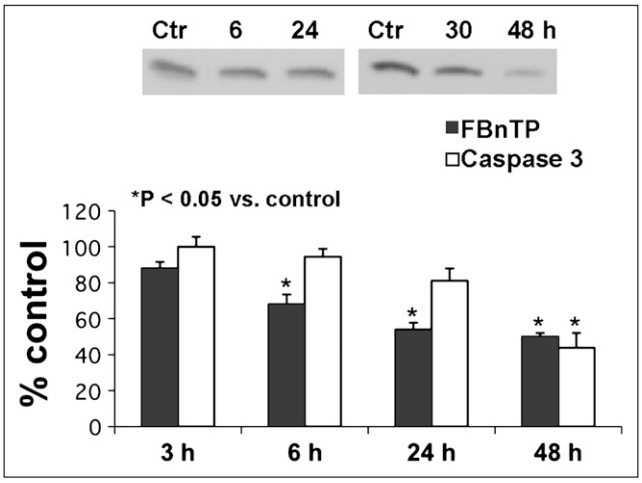

FIGURE 4. ^{18}F-FBnTP vs. caspase-3 activation. Significant increase in caspase-3 activation is observed after 48 h of paclitaxel treatment, lagging behind change in ^{18}F-FBnTP uptake. Ctr = nontreated cells.

in vivo assays in orthotopic prostate tumor. The potent proapoptotic taxane docetaxel induced a marked decrease of ^{18}F-FBnTP tumor uptake of more than 50%, and this effect was obtained within 48 h of treatment, a time point in which the effect on ^{18}F-FDG was marginal.

Both taxanes, paclitaxel and docetaxel, are dual-prong anticancer drugs, which induce mitotic arrest (due to microtubule stabilization) (*14,15*), and apoptotic cell death mediated by mitochondria (*16,17*). Paclitaxel toxicity is suppressed by the overexpression of antiapoptotic mitochondrial membrane proteins (e.g., Bcl-2, Bcl-x) and enhanced by proapoptotic proteins (e.g., Bax, Bad and Bak). Paclitaxel modulates the expression of Bcl-2 members, downregulates Bcl-2, and upregulates Bax (*18,19*). The present study provides additional validation for the apoptotic action of paclitaxel by demonstrating the linear increase of the Bax-to-Bcl-2 ratio and release of cytochrome c with increasing treatment duration.

$\Delta\Psi_m$ plays a key role in apoptotic cell death (*9,10*). In many cell lines, the initiation of apoptotic signaling is conditioned by permeabilization of the mitochondrial outer membrane and consequent collapse of $\Delta\Psi_m$. ^{18}F-FBnTP is a sensitive and accurate voltage sensor for detecting alterations in $\Delta\Psi_m$ (*13*). The uncoupling treatment protocol revealed that more than 80% of ^{18}F-FBnTP cellular uptake is driven by $\Delta\Psi_m$. Stepwise membrane depolarization, obtained by increasing extracellular potassium concentration, resulted in a linear decrease of ^{18}F-FBnTP cellular uptake, with a slope (a measure of probe sensitivity) and correlation coefficient (a measure of probe accuracy) nearly identical to those of the voltage sensor ^{3}H-tetraphenylphosphonium (*13*). ^{3}H-tetraphenylphosphonium is a standard tool for measuring $\Delta\Psi_m$ in vitro (*19,20*). Direct evidence for the capacity of ^{18}F-FBnTP to detect apoptosis was obtained by staurosporine, a common means for activating mitochondria-mediated apoptosis (*21,22*). In lung carcinoma cells, the

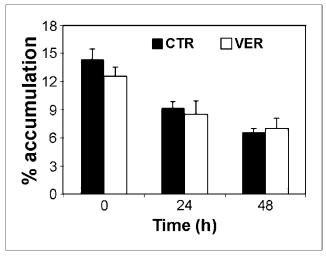

FIGURE 5. Effect of verapamil on ^{18}F-FBnTP uptake in cells treated for 24 and 48 h with paclitaxel. Verapamil did not induce any statistically significant effect on ^{18}F-FBnTP in either cell groups. Ctr = nontreated cells; VER = verapamil.

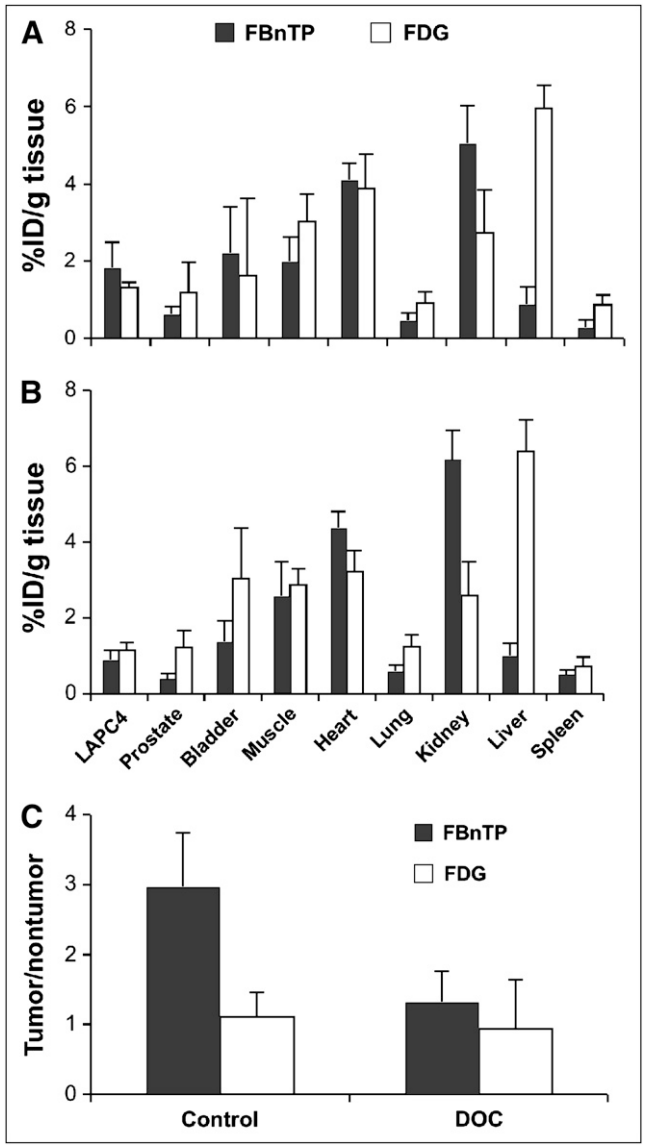

FIGURE 6. ^{18}F-FBnTP and ^{18}F-FDG biodistribution in prostate tumor–bearing mice, without (A) and with (B) docetaxel (DOC) 48-h treatment. Single clinical dose of docetaxel resulted in marked decrease in ^{18}F-FBnTP tumor-to-normal prostate uptake ratio, but small and insignificant effect was measured for ^{18}F-FDG (C). %ID/g = percentage injected dose per gram.

broadband protein kinase inhibitor staurosporine caused a marked decrease of ^{18}F-FBnTP cell-bound activity (*13*).

The time-dependent analysis performed in the present study supports the capacity of ^{18}F-FBnTP to quantify paclitaxel pharmacodynamics. Decreases in ^{18}F-FBnTP cellular uptake coincided in time and magnitude with the ratio of pro- to antiapoptotic proteins (Bax to Bcl-2), which regulate mitochondrial membrane permeabilization. A similar relationship was found between ^{18}F-FBnTP cellular uptake and release of cytochrome c. Both events—increased Bax expression and cytochrome c release—are known to coincide with $\Delta\Psi_m$ loss (*9,10*). In contrast, downstream activation of executioner caspase-3 lagged behind the initial decrease of ^{18}F-FBnTP cellular uptake. Other studies have reported a time frame of 36 h between time of exposure of cells to 20 nM paclitaxel and peak caspase-3 activation (*23,24*), which is similar to the time gap between 50 nM paclitaxel and caspase-3 activation found in the present study. The strong quantitative relationship with critical checkpoints of apoptosis suggests the promising potential of ^{18}F-FBnTP as an accurate tool for quantification of the efficacy and pharmacodynamics of proapoptotic drugs.

Lipophilic cations are potential substrates of efflux multidrug resistance proteins such as Pgp. Treatment with paclitaxel was shown to increase the expression of Pgp (*25*). Accordingly, a decrease in ^{18}F-FBnTP cellular uptake may be an outcome of Pgp overexpression, induced by paclitaxel. However, verapamil, a Pgp blocker (*26,27*), did not affect the accumulation of ^{18}F-FBnTP in MDA-MB-231 cells treated for 24 and 48 h with paclitaxel. The lack of effect of verapamil suggests that paclitaxel, given at a clinical dose of 50 nM, did not cause a significant change in Pgp expression, within a time frame of 48 h, and that the decline in ^{18}F-FBnTP cellular uptake is solely due to paclitaxel apoptotic action. This interpretation is in agreement with the absence of multidrug resistance proteins in the estrogen receptor–negative MDA-NB-321 cell line (*28*). Incubation of cells for 24 h with 100 nM paclitaxel was shown to increase Pgp expression in a drug-resistant cell line, but not in drug-sensitive ones (*29*). Alternatively, a lack of effect of verapamil may indicate a weak interaction of ^{18}F-FBnTP with Pgp, as demonstrated for other lipophilic phosphonium cations (*30*). Future studies will characterize the relationship between ^{18}F-FBnTP and multidrug resistance efflux proteins.

Potential Clinical Implications

Apoptotic cell death is a key mechanism involved in the etiology and pathology of numerous major diseases, such as diabetes, cancer, HIV and cardiac and degenerative disease. Importantly, apoptosis is the mechanism of action of many first-line chemotherapy agents. Despite the immense diagnostic significance, at the present time there is no effective molecular biomarker for early detection and quantitative assessment of the kinetics of the apoptotic process in target tissue using noninvasive means such as PET.

^{18}F-FDG is a viability tracer, and its efficacy in assessing tumor response to anticancer drugs was studied in numerous preclinical and clinical preparations, including breast cancer. A significant drop in breast tumor standardized uptake value, however, may occur late in the treatment, by the end of the first cycle of chemotherapy (*31*) and as early as 8 d after treatment in responders (*32*). The mechanisms contributing to the delay of ^{18}F-FDG response are still far from clear, but may be attributed to the unique metabolic plasticity of the regeneration of adenosine triphosphate by the cancer cell via both oxidative phosphorylation and glycolysis (*33,34*). The present study provides evidence that ^{18}F-FBnTP permits the detection of the apoptotic action of docetaxel earlier than that afforded by ^{18}F-FDG. ^{18}F-FBnTP uptake in the orthotopic prostate tumor dropped markedly within 48 h after administration of a clinical dose of docetaxel, whereas ^{18}F-FDG tumor uptake was hardly affected. Collapse of $\Delta\Psi_m$ is an early event, which takes place at the initiation of the apoptotic process. Several studies in cancer cells have shown that loss of $\Delta\Psi_m$ results in suppression of adenosine triphosphate synthesis via oxidative phosphorylation, followed by a compensatory increase of glucose breakdown via glycolysis, to balance the energy demand (*35,36*). This process suggests that in the presence of a proapoptotic agent, such as taxane, which initially causes $\Delta\Psi_m$ loss, ^{18}F-FDG tumor uptake might increase rather than decrease in the early phase of the treatment. A decrease in ^{18}F-FDG uptake in the tumor is expected to take place at later phases of the treatment, when glycolysis is slowed, energy reservoirs are depleted, and the cancer cell is near death. A recent study in colorectal cell lines reports an increase in ^{18}F-FDG cellular uptake in the first 24–48 h after incubation with several anticancer drugs (*37*). These data, corroborated by our findings, indicate the important advantage of targeting $\Delta\Psi_m$ using ^{18}F-FBnTP for the detection of apoptosis, earlier than that afforded by ^{18}F-FDG.

The tight quantitative correlation of ^{18}F-FBnTP with the evolution kinetics of apoptosis indicates the capacity of ^{18}F-FBnTP to address fundamental drawbacks of annexin V. Annexin V targets a short-lived event, PS externalization. The transient nature of PS externalization imposes 2 critical limitations. First, annexin V can provide an indication of whether apoptosis takes place but cannot report the cumulative effect and pharmacodynamics of the anticancer drug. Second, PS externalization occurs over a narrow time window, which may vary widely among individuals, drugs, and treatment protocols, as demonstrated for paclitaxel (*8*). Identifying the proper time to obtain a reliable estimate of the extent of apoptosis can be a challenge, when using annexin V SPECT or PET (*38*). In contrast, loss of $\Delta\Psi_m$ is an ongoing process not limited to a time window, which allows time-independent detection of apoptosis and monitoring of drug pharmacodynamics.

The high sensitivity of ^{18}F-FBnTP to detect apoptosis, and its capacity to report the progression over time of the metabolic defect may have important clinical implications in diseases other than cancer. Apoptotic cell death plays a

pivotal role in pathogenic processes in organs such as the heart and kidney. Whole-body PET scans acquired in dogs and mice have demonstrated the intense accumulation of ^{18}F-FBnTP in both organs (*13,39*). Recently, we have shown that ^{18}F-FBnTP cardiac uptake, documented by PET, is highly correlative with extent of apoptosis, as measured by terminal deoxynucleotidyl transferase biotin-dUTP nick end labeling staining (*40*). Progressive heart failure and reperfusion injury involve dynamic propagation of apoptotic cell death. Repeated ^{18}F-FBnTP PET scans can be an effective strategy for assessing the temporal and spatial kinetics of severity of the cardiac disease.

CONCLUSION

Targeting $\Delta\Psi_m$ using ^{18}F-FBnTP is a viable strategy for the early detection of apoptosis and for quantifying the evolution dynamics of apoptosis. This study focuses on the model system of taxanes and breast carcinoma cells, but the voltage sensor ^{18}F-FBnTP combined with PET may be an effective tool for assessing the kinetics of the effect of a wide spectrum of proapoptotic factors mediated by mitochondria and the efficacy of mitochondria-targeting therapeutic drugs.

REFERENCES

1. Holcik M, LaCasse EC, MacKenzie AE, Korneluk RG. *Apoptosis in Health and Disease: Clinical and Therapeutic Aspects.* Cambridge, U.K.: Cambridge University Press; 2006.
2. Duchen MR. Mitochondria in health and disease: perspectives on new mitochondrial biology. *Mol Aspects Med.* 2004;25:365–451.
3. Makin G, Hickman JA. Apoptosis and cancer chemotherapy. *Cell Tissue Res.* 2000;301:143–152.
4. Di Leo A. The European experience with docetaxel in the treatment of early-stage breast cancer. *Clin Breast Cancer.* 2002;3:S59–S62.
5. Galluzzi L, Larochette N, Zamzami N, Kroemer G. Mitochondria as therapeutic targets for cancer chemotherapy. *Oncogene.* 2006;25:4812–4830.
6. Tait JF. Imaging of apoptosis. *J Nucl Med.* 2008;49:1573–1576.
7. Blankenberg FG. In vivo detection of apoptosis. *J Nucl Med.* 2008;49(suppl 2): 81S–95S.
8. Mielke S. Individualized pharmacotherapy with paclitaxel. *Curr Opin Oncol.* 2007;19:586–589.
9. Pollack M, Phaneuf S, Dirks A, Leeuwenburgh C. The role of apoptosis in the normal aging brain, skeletal muscle, and heart. *Ann N Y Acad Sci.* 2002;959:93–107.
10. Susin SA, Zamzami N, Kroemer G. Mitochondria as regulators of apoptosis: doubt no more. *Biochim Biophys Acta.* 1998;1366:151–165.
11. Zamzami N, Kroemer G. The mitochondrion in apoptosis: how Pandora's box opens. *Nat Rev Mol Cell Biol.* 2001;2:67–71.
12. Madar I, Ravert H, Nelkin B, et al. Characterization of membrane potential-dependent uptake of the novel PET tracer ^{18}F-fluorobenzyl triphenylphosphonium cation. *Eur J Nucl Med Mol Imaging.* 2007;34:2057–2065.
13. Ravert HT, Madar I, Dannals RF. Radiosynthesis of 3-^{18}F-fluoropropyl and 4-^{18}F-fluorobenzyl triarylphosphonium ions. *J Labelled Comp Radiopharm.* 2004;47:469–476.
14. Schiff PB, Fant J, Horwitz SB. Promotion of microtubule assembly in vitro by taxol. *Nature.* 1979;277:665–667.
15. Manfredi JJ, Parness J, Horwitz SB. Taxol binds to cellular microtubules. *J Cell Biol.* 1982;94:688–696.
16. Ferlini C, Distefano M, Pignatelli F, et al. Antitumour activity of novel taxanes that act at the same time as cytotoxic agents and P-glycoprotein inhibitors. *Br J Cancer.* 2000;83:1762–1768.
17. Buchholz TA, Davis DW, McConkey DJ, et al. Chemotherapy-induced apoptosis and Bcl-2 levels correlate with breast cancer response to chemotherapy. *Cancer J.* 2003;9:33–41.
18. Tudor G, Aguilera A, Halverson DO, Laing ND, Sausville EA. Susceptibility to drug-induced apoptosis correlates with differential modulation of Bad, Bcl-2 and Bcl-xL protein levels. *Cell Death Differ.* 2000;7:574–586.
19. Lichtshtein D, Dunlop K, Kaback HR, Blume AJ. Mechanism of monensin-induced hyperpolarization of neuroblastoma glioma hybrid NG108-15. *Proc Natl Acad Sci USA.* 1979;76:2580–2584.
20. O'Brien TM, Carlson RM, Oliveira PJ, Wallace KB. Esterification prevents induction of the mitochondrial permeability transition by *N*-acetyl perfluorooctane sulfonamides. *Chem Res Toxicol.* 2006;19:1305–1312.
21. Scarlett JL, Sheard PW, Hughes G, Ledgerwood EC, Ku HH, Murphy MP. Changes in mitochondrial membrane potential during staurosporine-induced apoptosis in Jurkat cells. *FEBS Lett.* 2000;475:267–272.
22. Joseph B, Marchetti P, Formstecher P, Kroemer G, Lewensohn R, Zhivotovsky B. Mitochondrial dysfunction is an essential step for killing of non-small cell lung carcinomas resistant to conventional treatment. *Oncogene.* 2002;21:65–77.
23. Kumar D, Kirshenbaum L, Li T, Danelisen I, Singal P. Apoptosis in isolated adult cardiomyocytes exposed to adriamycin. *Ann N Y Acad Sci.* 1999;874:156–168.
24. Au JL, Kumar RR, Li D, Wientjes MG. Kinetics of hallmark biochemical changes in paclitaxel-induced apoptosis. *AAPS PharmSci.* 1999;1:E8.
25. Childs S, Yeh RL, Hui D, Ling V. Taxol resistance mediated by transfection of the liver-specific sister gene of P-glycoprotein. *Cancer Res.* 1998;58:4160–4167.
26. Herzog CE, Trepel JB, Mickley LA, Bates SE, Fojo AT. Various methods of analysis of mdr-1/P-glycoprotein in human colon cancer cell lines. *J Natl Cancer Inst.* 1992;84:711–716.
27. Beck WT, Qian XD. Photoaffinity substrates for P-glycoprotein. *Biochem Pharmacol.* 1992;43:89–93.
28. De Vincenzo R, Scambia G, Ferlini C, et al. Antiproliferative activity of colchicine analogues on MDR-positive and MDR-negative human cancer cell lines. *Anticancer Drug Des.* 1998;13:19–33.
29. Roberts JR, Allison DC, Donehower RC, Rowinsky EK. Development of polyploidization in taxol-resistant human leukemia cells in vitro. *Cancer Res.* 1990;50:710–716.
30. Gros P, Talbot F, Tang-Wai D, Bibi E, Kaback HR. Lipophilic cations: a group of model substrates for the multidrug resistance transporter. *Biochemistry.* 1992; 31:1992–1998.
31. Brindle K. New approaches for imaging tumour responses to treatment. *Nat Rev Cancer.* 2008;8:94–107.
32. Wahl RL, Zasadny K, Helvie M, Hutchins GD, Weber B, Cody R. Metabolic monitoring of breast cancer chemohormonotherapy using positron emission tomography: initial evaluation. *J Clin Oncol.* 1993;11:2101–2111.
33. Young CD, Anderson SM. Sugar and fat: that's where it's at—metabolic changes in tumors. *Breast Cancer Res.* 2008;10:202–210.
34. Rodríguez-Enríquez S, Gallardo-Pérez JC, Avilés-Salas A, et al. Energy metabolism transition in multi-cellular human tumor spheroids. *J Cell Physiol.* 2008;216:189–197.
35. Bashan N, Burdett E, Gumà A, et al. Mechanisms of adaptation of glucose transporters to changes in the oxidative chain of muscle and fat cells. *Am J Physiol.* 1993;264:C430–C440.
36. Ristow M. Oxidative metabolism in cancer growth. *Curr Opin Clin Nutr Metab Care.* 2006;9:339–345.
37. Sharma RI, Smith TA. Colorectal tumor cells treated with 5-FU, oxaliplatin, irinotecan, and cetuximab exhibit changes in ^{18}F-FDG incorporation corresponding to hexokinase activity and glucose transport. *J Nucl Med.* 2008; 49:1386–1394.
38. Mandl SJ, Mari C, Edinger M, et al. Multi-modality imaging identifies key times for annexin V imaging as an early predictor of therapeutic outcome. *Mol Imaging.* 2004;3:1–8.
39. Madar I, Ravert HT, Du Y, et al. Characterization of uptake of the new PET imaging compound ^{18}F-fluorobenzyl triphenyl phosphonium in dog myocardium. *J Nucl Med.* 2006;47:1359–1366.
40. Madar I, Gao D, Ravert HT, et al. ^{18}F-fluorobenzyl triphenyl phosphonium PET detects area-specific apoptosis in the aging myocardium [abstract]. *J Nucl Med.* 2007;4(suppl):166.